Journal of Physics: Conference Series **388** (2012) 012012 doi:10.1088/1742-6596/388/1/012012

Astrochemistry in an Ion Storage Ring

O Novotný[1,2], M H Berg[2], H Buhr[2,3] M Froese[2], W Geppert[4], M Grieser[2], F Grussie[2], M Hamberg[4], C Krantz[2], M Lestinsky[2], M Mendes[2], C Nordhorn[2], S Novotny[2], D A Orlov[2], A Petrignani[2], A Shornikov[2], J Stützel[2], D Schwalm[2,3], D W Savin[1] and A Wolf[2]

[1] Columbia Astrophysics Laboratory, Columbia University, New York, NY 10027, USA
[2] Max-Planck-Institut für Kernphysik, Saupfercheckweg 1, D-69117 Heidelberg, Germany
[3] Faculty of Physics, Weizmann Institute of Science, Rehovot 76100, Israel
[4] Department of Physics, Stockholm University, AlbaNova, SE-106 91, Stockholm, Sweden

E-mail: oldrich.novotny@mpi-hd.mpg.de

Abstract. Storage ring studies of low energy electron collisions with molecular ions have been carried out for dissociative recombination (DR) of fluorine-bearing molecules. Here we report on work aiming to improve the understanding of astrochemistry involving HF, a possible spectroscopic tracer of interstellar H_2. For CF^+ the rate coefficient was obtained for temperatures down to 10 K. For D_2F^+ the DR fragmentation branching ratios were determined to be 66(3)%, 24(2)%, and 10(2)% for the F+D+D, DF+D, and D_2+F channels, respectively. The molecular DR products of this reaction, DF and D_2, display an unusually high level of internal excitation, close to their dissociation limit.

1. Introduction

Molecules play an important role in the evolution of the cosmos from the formation of the first stars up to the present day. In the modern universe, they are a key component of diffuse, translucent, and dense molecular clouds; hot cores; photon dominated regions (PDRs); protostellar disks; protoplanetary disks; planetary and satellite ionospheres; cometary comae; and circumstellar envelopes around dying stars. As we strive to improve our understanding of these objects, it is necessary to be able to model and interpret their chemical composition, charge balance, emission and/or absorption spectra, and thermal structure. This, in turn, requires reliable knowledge of the underlying molecular collisions which control these properties.

Of particular astrophysical importance for electron-driven chemistry is dissociative recombination (DR) [1]. Using a triatomic molecule as an example, this reaction can proceed via the channels

$$\mathrm{e^- + ABC^+} \rightarrow \begin{cases} \mathrm{A + B + C} \\ \mathrm{AB + C} \\ \mathrm{AC + B} \\ \mathrm{BC + A.} \end{cases} \tag{1}$$

The energy gained from recombination is always greater than the dissociation energy required for at least one of these channels and so DR can proceed down to zero eV impact energies. DR is the primary neutralizing reaction for plasmas of less than a few thousand degrees K or electron

energies below a few eV. For chemical networks involving ion-molecule reactions, it is often the terminating step for particular synthesis pathways. Knowing branching ratios (BRs) for final DR products is critical as they can determine the viability of the pathway in question as well as whether or not a compound can be produced in the gas phase or if surface chemistry must be invoked. The end products of DR may also be energetic, in which case they can collisionally heat the plasma. Or they may be in excited states, in which case they can cool the gas through radiative relaxation.

Here we present a subset of results from recent experimental DR studies using the heavy-ion storage ring TSR at the Max-Planck-Institute for Nuclear Physics (MPIK) in Heidelberg, Germany. The goal of our work has been to improve the DR data used in astrochemical models for the molecular objects listed above and thereby improve our understanding of these sources. More specifically we have aimed to deepen our understanding of fluorine chemistry in the cold interstellar medium (ISM). This is a precondition for developing of a new proxy for H_2 abundance determinations in the cold ISM [2–4].

The rest of this paper is organized as follows: In Sec. 2 we discuss the chemistry of fluorine-bearing molecular ions. Their astrophysical importance is briefly given and shortcomings in the existing experimental DR rate coefficients are reviewed. In Sec. 3 we describe the TSR and the technological advances which allowed us to carry out improved measurements compared to previous work. In Sec. 4 we discuss results from DR studies on CF^+ and D_2F^+ and we summarize our findings in Sec. 5.

2. Astrochemistry of Fluorine

Although H_2 is the most abundant molecule in cold molecular clouds, direct observations are extremely difficult. Lacking a dipole moment, observations of this symmetric molecule typically rely on extremely weak ro-vibrational quadrupole transitions [5]. For this reason, in order to trace H_2 in the cold ISM, astrophysicists use proxies such as CO or HCN. Interestingly, recent theoretical astrochemical studies suggest that hydrogen fluoride, HF, can also serve as a proxy for H_2. Using HF as a tracer, however, requires an improved understanding of the underlying fluorine chemistry, particularly for the electron chemistry driven by DR.

Fluorine is unique among the elements in that HF is the only diatomic hydride formed by an exothermic reaction of a neutral atom with molecular hydrogen. This reaction has been extensively studied both theoretically and experimentally. Despite having a small activation barrier, it is expected to proceed rapidly at interstellar cloud temperatures ([6] and references therein). Based on this, a large fraction of interstellar fluorine is predicted to exist in the form of HF [7].

In fact, recent *Herschel* observations have revealed that HF comprises between 30% and 100% of the available F [8]. In some regions the HF abundance is greater than that of CO, even though the F nuclei abundance is $\approx 10^4$ times smaller than that of C nuclei. This suggests that HF may be a valuable tracer for molecular hydrogen in the cold ISM [3]. Proper use of HF for this purpose, however, requires an improved understanding of fluorine chemistry in molecular clouds [4].

One important destruction mechanism of HF in the cold ISM is

$$HF + C^+ \rightarrow CF^+ + H,$$

involving the readily ionized, abundant C-atoms. CF^+ has recently been detected by [9] and is predicted to be the second most abundant F-bearing molecule [7]. The main destruction mechanism of this system is DR via

$$e^- + CF^+ \rightarrow C + F. \quad (2)$$

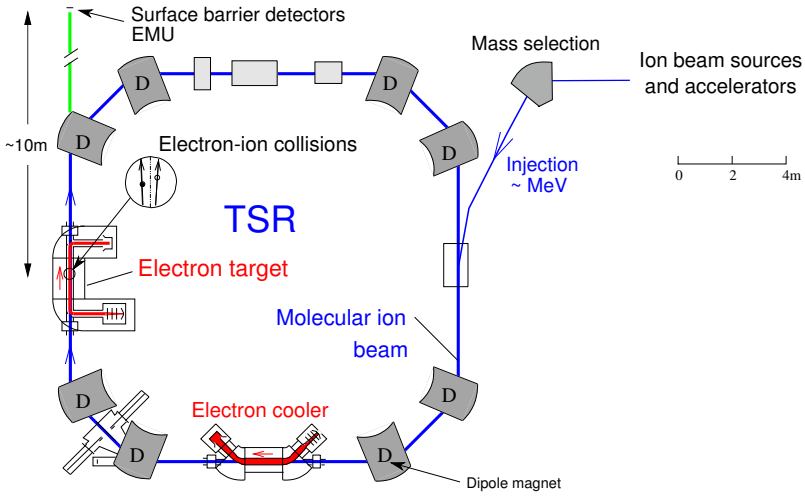

Figure 1. TSR experimental setup used for the DR work showing the dipole magnets (D) and other elements discussed in the text.

Thus, the DR rate determines whether fluorine stays locked in CF^+ or gets recycled to potentially form HF again.

Another HF destruction process is

$$HF + H_3^+ \rightarrow H_2F^+ + H_2.$$

This leads to the formation of H_2F^+. After formation, H_2F^+ can be destroyed by DR via

$$\begin{aligned} e^- + H_2F^+ &\rightarrow H + HF & (3)\\ &\rightarrow H_2 + F & (4)\\ &\rightarrow H + H + F. & (5) \end{aligned}$$

Two of the pathways recycle F (4 and 5) and one (3) leads to the HF again, thereby modifying the HF abundance for a given H_2 density. Thus reliable model HF abundances depend, in part, on an accurate knowledge of the relevant end product BRs for DR of H_2F^+.

While some previous DR work exists for the systems discussed above, a number of issues remain unresolved, warranting further experimental study. For CF^+ (reaction 2), the DR rate coefficient $\alpha(CF^+)$ has been measured using an ion storage ring [10]. These results extrapolated to lower temperatures were incorporated into models [4] which predict a CF^+ abundance in the Orion bar region ten times larger than observed [9]. This raises questions about both the quality of the experimental DR results and the validity of their extrapolation. DR of H_2F^+ (reactions 3–5) has been investigated using a flowing afterglow technique [11]. Unfortunately, these room-temperature results do not provide any information on the BRs for the outgoing channel and therefore the HF formation rate via DR of H_2F^+ remains unknown. It is clear that modeling the HF abundance in the cold ISM requires more reliable DR data than currrently exist for CF^+ and H_2F^+. This is discussed in more detail in [4] and [7].

3. The Heavy Ion Storage Ring TSR

With its ultra-high vacuum system at a base pressure of $\sim 10^{-11}$ mbar, TSR (see Fig. 1) is ideally suited to simulate the two-body collision regime important for interstellar gas-phase chemistry. Ions can be stored in TSR for tens of seconds at typical velocities of a few percent of the speed of light, corresponding to MeV energies. For molecules possessing a dipole moment, which is the case for all systems discussed here, this is typically long enough for the internal modes to radiatively relax to the ambient ring temperature of 300 K. Thus, most stored molecules will

decay to their $v = 0$ vibrational level before measurements begin. In a number of cases [12] the storage times are sufficient for also the rotational (J) populations to come into equilibrium with the ambient 300 K blackbody background. Thus the initial state of most stored ions will be similar to that for the cosmic molecular objects considered here. Typically among smaller species, it is only for homonuclear systems lacking a dipole moment, such as H_2^+ (but not HD^+), that the v and J states do not relax.

The TSR facility is equipped with two separate electron-ion merged beams sections referred to as the Cooler [13; 14] and the Target [15], respectively. Each provides a nearly monoenergetic (i.e., cold) electron beam that can be merged with the ion beam for ~ 1 m in two independent sections of the storage ring. During the first ~ 3 s of ion storage, both the Cooler and Target electron beams are velocity matched to the stored ions. Elastic collisions of the ions with the cold electron beam transfer energy from the recirculating ions to the single pass electrons, thereby reducing the energy spread of the ions [16]. This reduction contributes to the high energy resolution of the measurements. Electron cooling of the ions also reduces the ion beam diameter from ~ 40 mm to ~ 1 mm. This maximizes the efficiency of the finite-size detectors for collecting all end products and is important for fragment imaging experiments.

Energy-resolved DR measurements are performed by varying (i.e., detuning) the velocity of the Target electron beam while leaving the Cooler energy at cooling. The merging beam kinematics allows for an extremely precise adjustment of the relative detuning energy E_d, resulting in a much higher resolution DR measurements than is achievable by any other technique. The Target is normally operated employing a unique cryogenic photocathode as a source for extremely low velocity spread electrons [17; 18]. As a result TSR is the only facility past or present which is capable of reaching the sub-meV collision energies necessary to generate data for temperatures as low as ~ 10 K [19; 20].

Neutral DR products generated in the Target are unaffected by the first downstream dipole magnet. Instead of being deflected, they continue ballistically towards one of the dedicated DR detectors. Two of the various detectors used are described in Secs. 3.1 and 3.2.

3.1. Rate Coefficient Measurements

Rate coefficient measurements employ a Si surface-barrier detector with a 10×10 cm^2 active area. The detector pulse from each DR event is proportional to the total mass of impinging neutral fragments. The timing resolution is not sufficient for a single event to separate the individual fragment impacts from each other. For a DR event, where all fragments hit the detector, the pulse-height corresponds to the full mass of the parent ion. Background processes typically produce at least one charged end product which is deflected by the first dipole magnet downstream of the Target and does not reach the DR detector. The resulting pulse corresponds to a lower total mass thus allowing DR to be easily distinguished from background.

Using TSR we measure the DR cross section σ_DR times the relative collision velocity v_r convolved with the energy spread of the experiment at a given E_d, yielding an experimental rate coefficient $\langle \sigma_\mathrm{DR}\, v_\mathrm{r} \rangle$. Its value is determined from

$$\langle \sigma_\mathrm{DR}\, v_\mathrm{r} \rangle = \frac{R_\mathrm{DR}\; v_\mathrm{i}\; e}{L\; n_\mathrm{e}\; I_\mathrm{i}}, \tag{6}$$

where R_DR is the DR event count rate at the detector, v_i is the velocity of the ion beam in the laboratory frame, e is the elementary charge, L is the length of the electron-ion interaction region in the Target, n_e is the electron density, and I_i is the ion beam current. The electron density is determined from the measured electron beam current, energy, and cross sectional area.

Usually the rate coefficient is first determined for all detuning energies on a relative scale only. For this the relative ion current is monitored by measuring the rate of background events caused by collisions of the ion beam with residual gas. The absolute scaling of $\langle \sigma_\mathrm{DR}\, v_\mathrm{r} \rangle$ versus

$E_{\rm d}$ is then set by measuring $I_{\rm i}$ at a single energy. For strong beams this can be done using a DC current transformer [21]. For weak beams we use a recently developed beam lifetime measurement technique to directly determine $\langle \sigma_{\rm DR}\, v_{\rm r} \rangle$ at a fixed energy. This method is based on a determination of the ion beam lifetime in a separate set of measurements. The detector count rate, which is directly proportional to I_i, is monitored as a function of storage time. When the Target beam is switched on (and set to a fixed energy) we measure the decay rate of the stored ions $\lambda^{(\rm on)}$. This is due to both DR and background processes. With the Target off we measure a decay rate $\lambda^{(\rm off)}$ due only to background. These can be combined to yield

$$\langle \sigma_{\rm DR}\, v_{\rm r} \rangle = \frac{\lambda^{(\rm on)} - \lambda^{(\rm off)}}{n_{\rm e} L/C} \tag{7}$$

where C is the TSR circumference. This normalization method is discussed in more detail in [22]. Using it results in accuracies of better than 20%.

To generate a thermal rate coefficient α, such as usually needed in astrophysics, we must first deconvolve our $\langle \sigma_{\rm DR}\, v_{\rm r} \rangle$ results to extract $\sigma_{\rm DR} v_{\rm r}$. This can convolve with a Maxwell-Boltzman velocity distribution to yield the thermal rate coefficient versus plasma temperature. Given the experimentally accessible energy range we are able to generate reliable values of α for temperatures from $\sim$10 K up to temperatures where the vibrational excitation of the molecule can be neglected, typically several 1000 K.

3.2. Fragmentation and final-state branching ratios

DR occurs on the time scale of $\sim$fs which is very short compared to the $\sim\mu$s time-of-flight of the fragments to the DR detectors. The kinetic energy released (KER) in DR causes the neutral fragments to move apart and by the time they reach the detector they can be separated by several centimeters. We take advantage of this to investigate the various possible outgoing channels of the DR process.

Branching ratio measurements are performed using an Energy-sensitive MUltistrip (EMU) detector. This newly-developed, Si surface barrier detector has a position sensitivity of $\sim$ 0.08 cm and a maximum count rate of $\sim$ 1.5 kHz [23]. EMU provides information on the impact positions and the number of outgoing fragments. The signal pulse amplitude of each impact provides information on the mass of the detected fragment. From this information we are able to assign the fragmentation channel for each DR event and thereby the BR for various fragmentation channels. Highly precise BR can be obtained from only a few thousands detected DR events.

The EMU detector also allows us to study the final-states of DR products. The spatial positions of the fragment impacts reveal the kinetic energy released (KER) in the DR event. The exothermicity for each possible final state of the fragments can readily be calculated from known atomic and molecular constants. Taking all this information together, the KER distributions for the various outgoing fragmentation channels can be translated to the internal excitation distributions of the DR products or/and of the parent ions. Information for specific BRs can then be derived by comparing the spatial information from EMU to the predicted impact pattern of the various initial and final states. Utilizing EMU, fragmentation and final-state BRs as well as excitation of parent ions, have already been successfully determined for several systems such as D_2H^+ [23] and D_3O^+ [24; 25].

4. Results

Here we present representative results from recent experimental investigations of DR for CF^+ and D_2F^+. A full account of our findings for these two systems will be given elsewhere.

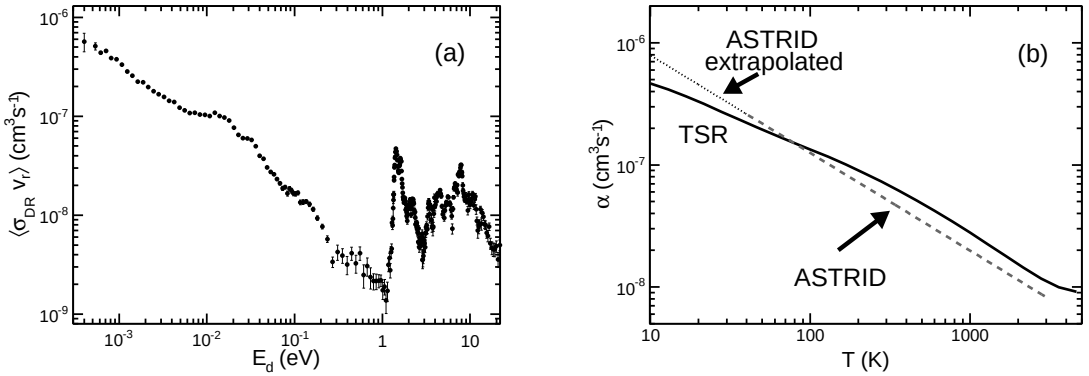

Figure 2. DR of CF^+. **(a)** Experimental rate coefficient $\langle \sigma_{\rm DR}\, v_{\rm r} \rangle$ versus detuning energy $E_{\rm d}$. **(b)** Thermal rate coefficient α versus plasma temperature T. The full curve shows our results and the dashed curve those of ASTRID [10]. The dotted line indicates the extrapolation of the ASTRID data to low T.

4.1. A new, low-temperature plasma rate coefficient for DR of CF^+

CF^+ was produced by stripping CF_3^- to CF^+ in the MPIK tandem accelerator and stored in the ring at 3.0 MeV. Low-energy DR of CF^+ produces C and F fragments with a maximal kinetic energy release of 3.4 eV and the corresponding distances fit well into the 10×10 cm^2 detector at TSR. The data were acquired at storage times 3–35 s after the ion injection. The experimental rate coefficient $\langle \sigma_{\rm DR}\, v_{\rm r} \rangle$ is displayed in figure 2a, while the resulting thermal rate coefficient is plotted in figure 2b. The data agree reasonably well with previous results from the ASTRID storage ring [10]. The TSR results, however, extend to temperatures as low as 10 K, which are most relevant for interstellar cloud chemistry. Extrapolating the ASTRID data to these low temperatures introduces a discrepancy of a factor of ~ 2. This demonstrates the advantage of the $\sim$ 20-fold improved collision energy resolution at the TSR provided by the photocathode-produced electron beam.

4.2. Fragmentation BR and excitation of DR products for D_2F^+

The maximal KER of the two-fragment channels for H_2F^+ DR at $E_{\rm d} = 0$ eV are 7.2 and 8.6 eV for reactions 4 and 3, respectively. This can result in large distances of the DR products at the detector. Such fragment impact positions could exceed the size of our detectors by $\approx 50\%$ which would make the interpretation of the data impossible. To solve this problem we have used the isotopologue D_2F^+ for our DR measurements. The resulting DR fragments are heavier which guarantees a narrower dissociation cone and therefore 100% geometrical detection efficiency.

D_2F^+ was produced in a hollow-cathode ion source using a mixture of D_2 and CF_4. The ion beam was accelerated by a Pelletron accelerator to 2.5 MeV, injected into TSR, and further accelerated to 4.1 MeV. Data were acquired using the EMU detector at storage times of 6–20 s after ion injection.

The fragmentation BRs obtained at zero detuning energy are 66(3)%, 24(2)%, and 10(2)% for the F+D+D, DF+D, and D_2+F channels, respectively. Given the energy spread of the electron beam this energy corresponds to a plasma temperature of 10 K. These BRs do not change significantly at the higher detuning energies studied which correspond to plasma temperatures up to $\sim$ 400 K. The error bars provided represent their estimated upper limits; a more detailed analysis including minor corrections would provide more precise BR values with reduced errors.

For each fragmentation channel we have determined the KER distribution from the fragment distances at the detector. In figure 3a we show the analysis procedure for the DF+D channel.

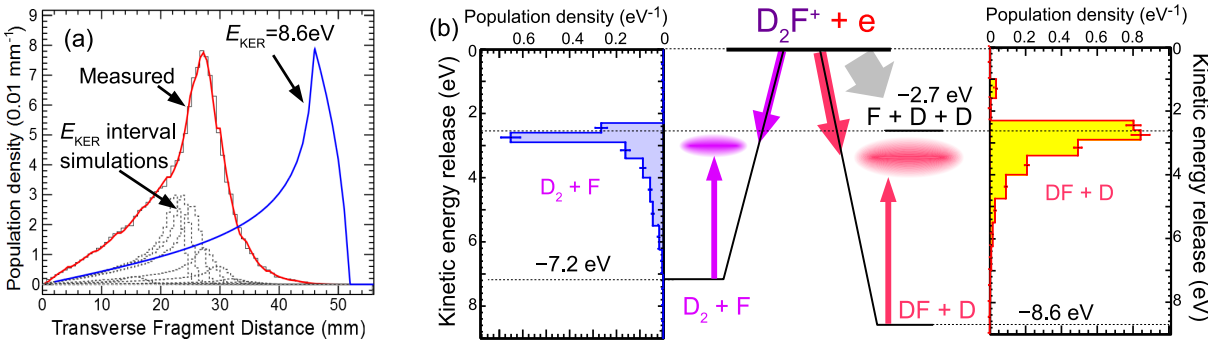

Figure 3. (Color online) **(a)** Transverse fragment distance distribution for $D_2F^+ + e^- \rightarrow DF + D$ at $E_d = 0$ eV. The unbroken black line histogram shows the measured data and the dashed lines the simulated fragment distance distributions for various E_{KER} intervals. The amplitudes of the simulations have been adjusted to give the red curve as a fit to the measured data. The blue curve shows the expected results for a $E_{KER} = 8.6$ eV forming DF and D in their ground state. **(b)** Energy diagram relevant for the DR of D_2F^+ together with the measured KER distributions for each two-body DR channel. The potential energies for ground state products are negative with respect to the ground state of $D_2F^+ + e^-$ for all three possible fragmentation channels. Their absolute values give the maximum KER available. The product internal excitation is therefore reflected by the difference between the maximum possible and the measured KER.

The resulting KER distributions for both the DF+D and D_2+F channels are displayed in figure 3b. For both channels the measured KERs are significantly lower than those expected for ground state DR products. A sharp maximum KER is seen near $\sim$ 2.7 eV. Neither D nor F have electronic states in this energy range. Additionally the excitation of the parent ion is < 0.04 eV (obtained from the KER distribution of D+D+F, not shown here). Thus the low KER for both two-body channels indicate a high level of internal excitation in the molecular products DF and D_2. KERs of less than 2.7 eV in the two-body channels results in excitation of DF and D_2 fragments above their respective dissociation limits. Hence the two body channels turn off for KER < 2.7 eV and the system dissociates into fully atomic D+D+F.

5. Discussion and Summary

The new DR plasma rate coefficient for CF^+ significantly corrects the values previously used at the low temperatures relevant for interstellar cloud chemistry. DR is the dominant destruction channel for CF^+ in these environments. Therefore the lower α will result in higher CF^+ abundances predicted by the astrochemical models. This will further increase the discrepancy between these models and observations [4]. Our result suggests that the origin of this discrepancy lies in the CF^+ production rather than its destruction.

The fragmentation BRs for DR of fully deuterated and fully hydrogenated isotopologues usually do not differ significantly (see, e.g., H_3O^+ and D_3O^+ [26]). Our D_2F^+ results should therefore also be applicable to H_2F^+. The new experimental BRs show that DF(HF) fragments are produced in 24% of the DR events. Existing astrochemical models assume 50% for this channel and therefore overestimate the HF abundance. We plan to implement our DR results for both CF^+ and D_2F^+ (H_2F^+) into models for the fluorine chemistry of interstellar clouds in order to quantify the effects on the predicted fractional [HF]/[H_2] abundance.

The internal excitation of the DF and D_2 products from low-energy DR of D_2F^+ is the most extreme case found so far among the polyatomic molecules investigated (see, e.g., D_2H^+ [23]

or D_3O^+ [24]). Excitation close to the dissociation limit suggests strong contributions of a two-step DR process, where the molecular DR products are initially excited above their first dissociation threshold and then rapidly decay to form the three-body channel. We are presently analyzing the dissociation geometries in the D+D+F channel to look for this process. The high excitation of the molecular products also suggests that DR of D_2F^+ (H_2F^+) might effect the energy balance in interstellar clouds. Instead of releasing the binding energy as kinetic energy of the DR fragments (heating the cloud), the energy is stored as molecular excitation and later released by radiation, eventually escaping the cloud.

Acknowledgments
We thank the MPIK accelerator and TSR crews for their excellent support. ON and DWS were supported in part by the NSF Division of Astronomical Sciences Astronomy and Astrophysics Grants program and by the NASA Astronomy and Physics Research and Analysis Program. DS acknowledges the support of the Weizmann Institute of Science through the Joseph Meyerhoff program. The work is supported in part by the German-Israeli Foundation for Scientific Research [GIF under contract nr. I-900-231.7/2005]. WG acknowledges partial support by the COST Action CM0805: "The Chemical Cosmos: Understanding Chemistry in Astronomical Environments".

References

[1] Geppert W D and Larsson M 2008 *Mol. Phys.* **106** 2199–2226
[2] Sonnentrucker P, Friedman S D and York D G 2006 *Astrophys. J.* **650** L115–L118
[3] Sonnentrucker P *et al.* 2010 *Astron. Astrophys.* **521** L12
[4] Neufeld D A and Wolfire M G 2009 *Astrophys. J.* **706** 1594–1604
[5] Luhman M L, Jaffe D T, Keller L D and Pak S 1994 *Astrophys. J.* **436** L185–L188
[6] Zhu C, Krems R, Dalgarno A and Balakrishnan N 2002 *Astrophys. J.* **577** 795–797
[7] Neufeld D A, Wolfire M G and Schilke P 2005 *Astrophys. J.* **628** 260–274
[8] Neufeld D A *et al.* 2010 *Astron. Astrophys.* **518** L108
[9] Neufeld D A *et al.* 2006 *Astron. Astrophys.* **454** L37–L40
[10] Novotný O *et al.* 2005 *J. Phys. B* **38** 1471–1482
[11] Adams N G and Smith D 1988 *Chem. Phys. Lett.* **144** 11–14
[12] Wolf A, Buhr H and Novotn O 2011 *J. Phys. Conf. Ser.* **300** 012008
[13] Steck M *et al.* 1990 *Nucl. Instr. Meth. A* **287** 324–327
[14] Pastuszka S *et al.* 1996 *Nucl. Instr. Meth. A* **369** 11–22
[15] Sprenger F *et al.* 2004 *Nucl. Instr. Meth. A* **532** 298–302
[16] Poth H 1990 *Phys. Rep.* **196** 135–297
[17] Orlov D A *et al.* 2004 *Nucl. Instr. Meth. A* **532** 418–421
[18] Orlov D A *et al.* 2009 *J. App. Phys.* **106** 054907
[19] Kreckel H *et al.* 2005 *Phys. Rev. Lett.* **95** 263201
[20] Schmidt E W *et al.* 2007 *Phys. Rev. A* **76** 032717
[21] Unser K 1981 *IEEE Trans. Nucl. Sci.* **28** 2344–2346
[22] Kreckel H *et al.* 2010 *Phys. Rev. A* **82** 042715
[23] Buhr H *et al.* 2010 *Phys. Rev. A* **81** 062702
[24] Buhr H *et al.* 2010 *Phys. Rev. Lett.* **105** 103202
[25] Novotný O *et al.* 2010 *J. Phys. Chem. A* **114** 4870–4874
[26] Neau A *et al.* 2000 *J. Chem. Phys.* **113** 1762